

Phase-Transfer Model for the Dynamics of “Micellar Autocatalysis”

T. Buhse, R. Nagarajan,[†] D. Lavabre, and J. C. Micheau*

Laboratoire des IMRCP, UMR au CNRS N° 5623, Université Paul Sabatier, 118, route de Narbonne, F-31062 Toulouse Cedex, France

Received: February 17, 1997; In Final Form: March 26, 1997[⊗]

The biphasic alkaline hydrolysis of ethyl caprylate (EC) exhibits highly nonlinear kinetics that has been attributed in the literature to “micellar autocatalysis” (Bachmann, P. A. et al. *Nature* **1992**, 357, 57). New experimental results enable us to establish a macroscopic kinetic model quantitatively accounting for the dynamics of this reaction. According to the model, EC is carried from the organic to the aqueous phase by a transient micelle–EC complex (MEC). Curve fitting of the experimental kinetic data by inverse treatment shows that the formation of MEC is more favorable than that of the pure caprylate micelles (M) and occurs at a critical concentration that is smaller than the cmc associated with the formation of M. We demonstrate, in contrast to previous claims, that classical micellar catalysis is not involved in the overall reaction process, but the observed nonlinear kinetics is a consequence of the dynamics of the MEC-mediated phase-transfer reaction.

I. Introduction

Chemical systems in which molecular aggregates such as micelles or vesicles have been reported to catalyze their own formation have attracted considerable scientific interest in the recent years.^{1–8} A prominent example of such processes has been reported by Bachmann, Luisi, and Lang in 1992.³ In this case, the biphasic alkaline hydrolysis of an ester shows highly nonlinear kinetics that has been attributed to the effect of micellar autocatalysis. In this reaction, ethyl caprylate (EC), which is practically immiscible with water, undergoes alkaline hydrolysis when placed in contact with an underlying aqueous solution of 3 M NaOH. The reaction yields amphiphilic sodium caprylate, which is known to form anionic micelles in aqueous media.

The first stage of the reaction is characterized by a pronounced induction period, i.e., a very slow formation of caprylate ions (C) apparently due to the spontaneous reaction between EC and OH[−] taking place solely at the interface between the two liquid phases. As suggested by the above authors,³ after the concentration of C reaches the cmc, which was given to be at 0.1 M, the reaction takes off dramatically and ends abruptly when after about 33 h EC is entirely consumed to give a single transparent phase. The caprylate micelles are believed to catalyze the alkaline hydrolysis of EC, that is, the nucleophilic attack of OH[−] (present in the aqueous phase) on EC (located in the micellar phase). However, this suggestion contradicts some basic features of micellar catalysis, namely, that aqueous anionic micelles are known to inhibit but not catalyze reactions of nonionic organic substrates with anions.^{9,10} This is readily explained by the incorporation of the substrates into the hydrophobic micellar core and the exclusion of the anions from the anionic micellar surface because of electrostatic repulsion.^{11,12}

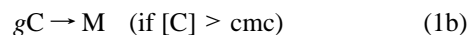
However, C monomers, which are the building blocks of the micelles, are obviously produced by an autocatalytic pathway in the course of this reaction. A purely qualitative interpretation has led to the conclusion that the micelles catalyze their own

formation. This hypothesis has been designated by the authors³ as “autopoietic self-replication” of micelles and discussed with respect to the basic chemical mechanisms of life. Besides this far reaching point of view, the kinetic curves of the formation of C and of the micelles show without any doubt the signature of highly nonlinear dynamics. This aspect should be the subject of a more detailed explanation.

By using exclusively the experimental results of Bachmann, Luisi, and Lang,³ several authors^{13–16} have attempted to describe the mechanism of the reaction system and have proposed different kinetic models. All models describe the autocatalytic formation of C in the framework of micellar catalysis as cited above. These models are briefly recalled below (split into 2 main groups referred to as type A and type B models).

Type A models explicitly include an a priori set cmc value and make no attempt to describe the aggregation process. The representation of the overall reaction is artificially divided into two parts. The first part corresponds to a domain where [C] < cmc, which is a priori assumed to be equivalent to the induction period. The second part corresponds to a domain where [C] > cmc, which is a priori assumed to be equivalent to the stage of rapid product formation. Consequently, the kinetic schemes change their structures when switching from the first to the second stage, resulting in two different kinetic descriptions for the same overall reaction.

This approach has been applied by Billingham and Coveney¹³ to the following kinetic scheme (called by them “model with known cmc”):



where step 1a denotes the uncatalyzed formation of the surfactant, step 1b the formation of micelles M, which is treated to be of first order and considered not reversible, and step 1c the catalytic formation of C in the presence of the micelles (g is the average aggregation number of the micelles). In the case where [C] ≤ cmc, the rate of step 1b is set equal to 0; i.e., catalytic step 1c is only operative if [C] > cmc. Any influences of the reactions on the aggregation process do not fall within the scope of this approach.

[†]Permanent address: Department of Chemical Engineering, The Pennsylvania State University, University Park, PA 16802.

* To whom correspondence should be addressed. E-mail: micheau@gdp.ups-tlse.fr.

[⊗] Abstract published in *Advance ACS Abstracts*, May 1, 1997.

Using the type A approach, a more specific kinetic description taking into account the biphasic character of the reaction system has been proposed by Chizmadzhev et al.¹⁴ The authors treat the reaction strictly as a surface process in which the accelerating effect of product formation is assumed to be due to the growth of the organic/aqueous interface.¹⁷ The first part is assumed to be the uncatalyzed hydrolysis occurring solely at the macroscopic interface. The second part is assumed to be the catalyzed formation of C proceeding at the microscopic micellar/aqueous interface. For that reason the kinetic description includes the absorption of EC at the micellar surface, which is represented by a complex formation between EC and the micelle. However, this process is not believed to affect the aggregation.

The models of type A remain unsatisfactory from a more rigorous dynamical point of view, since they operate with an a priori fixed threshold concentration (the cmc) of which the model can give no description.

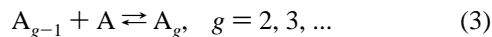
Type B models consist of a *single* set of rate equations for the entire process in contrast to type A models, which require two sets of rate equations corresponding, respectively, to the two domains identified a priori as the induction period and the product formation stage.

A first attempt in this direction has been reported by Billingham and Coveney¹³ by a scheme (designated by them as “clock reaction model”) that includes steps 1a and 1b, which in this model is operative without a prefixed threshold concentration:



The main dynamic feature of the model originates from step 2, which is treated to be of third order and denotes a cubic autocatalysis.¹⁸ In this process formally two caprylate micelles are considered to react with g molecules of EC to yield three caprylate micelles. Clearly, this step represents a simplification that allows no detailed understanding of the catalytic process. Furthermore, the model does not generate a cmc, since the aggregation of C—step 1b—is treated again as an irreversible first-order process. However, model calculations show good qualitative agreement with the entire kinetic curve given in ref 3. This indicates that the reaction displays a dynamic behavior *similar* to a chemical clock reaction,^{18,19} which can be expressed by a cubic overall (empirical) rate law.

As recently demonstrated by Coveney and Wattis,¹⁵ type B models can also give a description of the aggregation process and consequently generate the cmc in a self-consistent manner. Their model is based on a generalized Becker–Döring scheme²⁰ that was applied to a multistep micellar aggregation process:



where A_g denotes an aggregate containing g monomers. This process is quite similar to that given in the theory of Aniansson and Wall.^{21–23} By rigorous contraction of the Becker–Döring description, the authors finally arrived at a kinetic scheme including steps 1a and 1c and a one-step micellization equilibrium 4 that is treated to be of g th order:

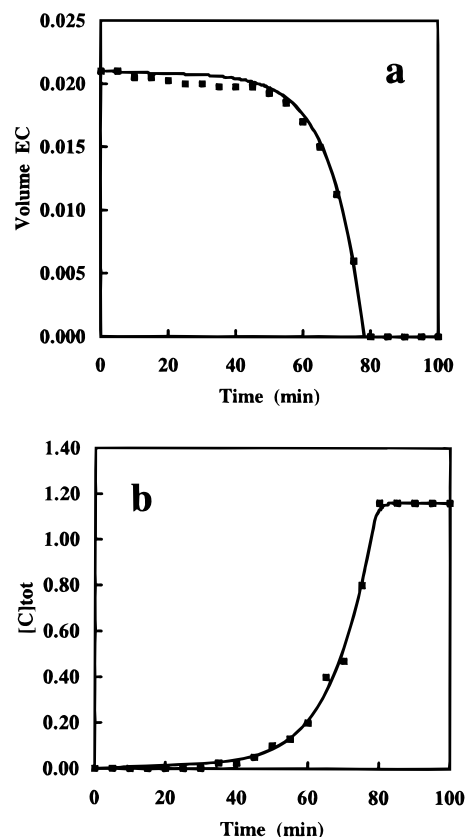


Figure 1. Biphasic alkaline hydrolysis of EC (a) time evolution of EC (total volume of overlaid organic phase in L) and (b) time evolution of C (total concentration in aqueous phase in mol L⁻¹): (■) experimental points; (—) fitting by the kinetic model as shown in Scheme 1. See Appendix II for the kinetic parameters.

where $g = 63$ corresponds to the average aggregation number of C aggregates as given in ref 3. Process 4 is equivalent to the one-step mass action model²⁴ of micellar aggregation. However, the model directly implies a catalysis by the pure caprylate micelles (step 1c), which is unrealistic from a chemical point of view (micelles attract EC but repel OH⁻, leading to an inhibition of the hydrolysis). Furthermore, this model cannot reproduce the specific kinetic curve of C formation and that of EC consumption, which we have observed experimentally (Figure 1).

In contrast to the models in the literature that are based on micellar catalysis, we present in this paper a kinetic model of type B that describes the reaction in terms of the well-known transport phenomenon of phase transfer. The model leads to a quantitative description of the overall reaction and shows that pure caprylate micelles indeed do not account for the autocatalytic kinetics.

We apply the method of inverse treatment, which allows us to assign the model directly to experimental data and to exclude or validate a proposed mechanism by its capacity to fail or fit experimental data. In this respect, we must point out that the kinetic data of this reaction as given in the literature³ are not adequate for a thorough dynamic analysis because of the lack of a sufficient number of well-situated experimental points.

II. Experimental Results

To obtain sufficient kinetic information required for the modeling, first we reinvestigated the kinetics of the biphasic hydrolysis of EC by measuring simultaneously the time evolution of EC and C. Second, we determined the cmc of sodium caprylate in 3 M NaOH solution by tensiometry, and third, we

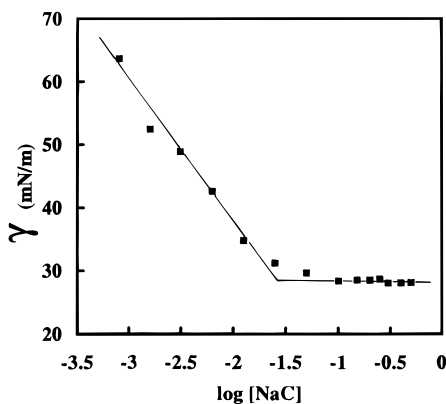


Figure 2. Variation of the surface tension (γ) with log of the concentration of sodium caprylate ($[\text{NaC}]$) in aqueous 3 M NaOH at 25 °C indicating a cmc of ~ 0.02 M.

measured the solubility of EC in a micellar solution of sodium caprylate in the presence of NaCl and ethanol.

Reaction Kinetics. The biphasic alkaline hydrolysis of EC was carried out under the same conditions and initial reactant concentrations as originally reported.³ In our case, more vigorous mixing of the two liquid phases consisting of 70 mL of aqueous 3 M NaOH and 21 mL of neat ethyl caprylate resulted in a considerable reduction in the total reaction time from 33 h to about 80 min (see Figure 1). This effect, depending on the stirring rate, the stirrer size, and the specific geometrical properties of the reaction vessel, indicates that the system shows a distinct sensitivity toward the mixing intensity.

The kinetic curves for the consumption of EC and the formation of total C (Figure 1) have been measured by the use of two independent methods. They show a significant dynamical characteristic that may be overlooked while the plotted time evolution of C in ref 3 is viewed. In particular, we observe a comparatively smooth increase of C formation after the induction period, which is followed by a truly abrupt cutoff of the reaction after about 80 min.²⁵

Critical Micelle Concentration. The cmc of sodium caprylate in 3 M NaOH was determined by tensiometric method to be ~ 0.02 mol L⁻¹ (Figure 2), which is also in agreement with the predictions of the a priori theory of Nagarajan and Ruckenstein²⁶ (see Appendix I). This value is considerably lower than those given in the literature for aqueous solutions of sodium caprylate without added electrolyte, which were found to be approximately about 0.35 mol L⁻¹.^{11,27} The difference among the cmc values arises from the well-known effect of

added electrolyte, which lowers the cmc by causing a decrease in the repulsion between the polar head groups at the micelle surface.²⁸ Control experiments have shown that equimolar addition of ethanol (which will be found in the aqueous phase of the reaction system at the same concentration as C and which may have an effect on the cmc and on the micelle size) does not have a significant effect on the cmc.

Solubility of EC in the Micellar Phase. The uptake of EC into the micellar phase of C aggregates in the presence of 3 M NaCl and 0.1 M ethanol has been measured (Figure 3a). In our study the attempted dissolution of 0.002–0.015 mol L⁻¹ EC in the aqueous solution of 0.1 M sodium caprylate resulted in a saturation value of 0.011 mol L⁻¹ EC, i.e., EC/sodium caprylate ≈ 0.11 .

III. Kinetic Model

To account for the above experimental results, a kinetic model that represents adequately the dynamic nature of this type of reaction is presented. This model can quantitatively reproduce the experimentally observed kinetics of C formation and EC consumption and explains the effect of apparent micellar autocatalysis by the features of a transport phenomenon that is related to the biphasic character of the reaction system.

The formulation of the model follows a heuristic approach, with the experimental results of section II providing a strong basis. By reasoning similar to that already stated by Coveney and Wattis,¹⁵ we included a one-step micellization process of the mass action type²⁴ in the model. We have confirmed by numerical testing of a multistep aggregation equilibrium (considering aggregation numbers $g \leq 160$) that this simplification is satisfactory for our macroscopic approach in the framework of this contribution. This includes the capacity of the model to generate the cmc in a self-consistent manner, i.e., by its own structure.

Using a one-step micellization process requires a knowledge of the average aggregation number g , which has to be introduced into the model. On the basis of an a priori molecular thermodynamic theory, we predicted this value to be $g \approx 40$ for caprylate micelles under specific reaction conditions (see Appendix I). The predictions from the theory of micelles are plotted in Figure 4 showing the size distribution of aggregates at different total concentrations of C. One can observe the very narrow dispersion of sizes, which justifies the simplification of a single population of micelles. We note here that the specific numerical value used for the micellar aggregation number does

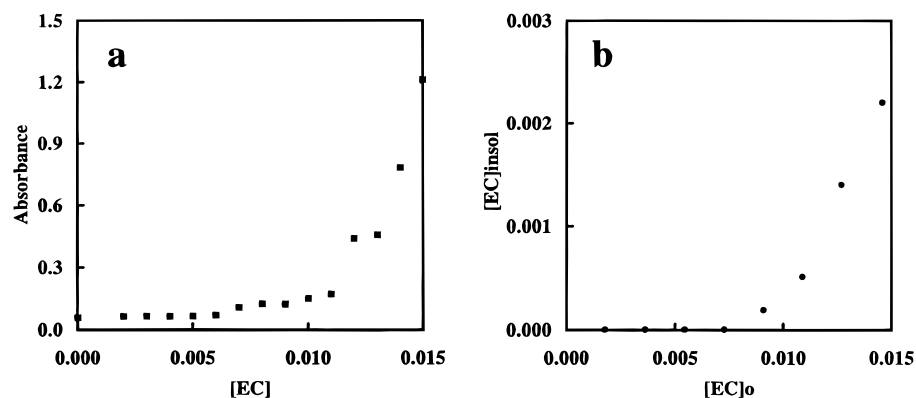


Figure 3. Solubility of EC in an aqueous solution of 0.1 M sodium caprylate (NaC) + 3 M NaCl at 25 °C: (a) experimentally determined by turbidimetric measurement at $\lambda = 400$ nm indicating a maximum solubility of EC of 1.1×10^{-2} mol L⁻¹; (b) simulated by the kinetic model (Scheme 1) and by using the kinetic parameters obtained by the fitting of experimental data (Appendix II) where the simulation runs under the conditions $[\text{OH}^-]_0 = 0$. $[\text{EC}]_{\text{insol}}$ denotes the concentration of initial ethyl caprylate ($[\text{EC}]_0$) that remains at the interface after the system has reached equilibrium.

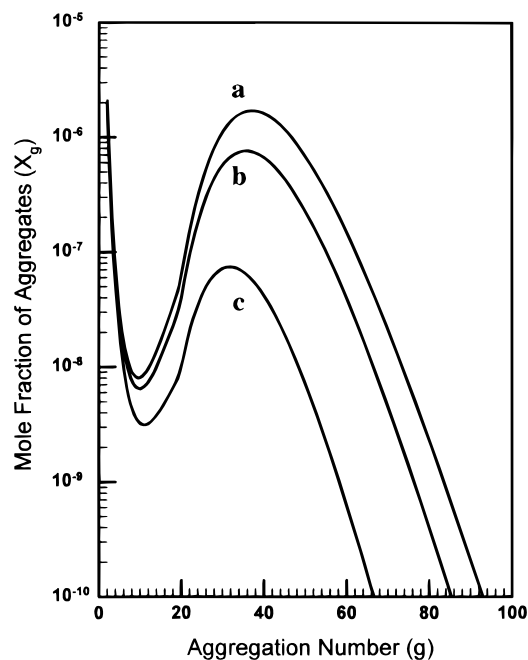
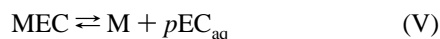
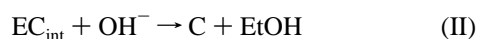
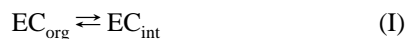


Figure 4. Predicted equilibrium size distribution of C aggregates at 90 °C and 3 M NaCl (see Appendix I). Total concentrations of C are (a) 0.1045, (b) 0.0576, and (c) 0.026 mol L⁻¹.

SCHEME 1: Sequence Network of the Kinetic Model for the Biphase Alkaline Hydrolysis of EC^a



^a EC_{org} = bulk organic phase. EC_{int} = portion of EC at the organic/aqueous interface. C = caprylate monomers (present in the aqueous phase). M = micelles consisting of g monomers ($g = 40$). MEC = micelle-EC complex containing $p = 5$ molecules of EC. EC_{aq} = portion of EC present in the aqueous phase. EtOH = ethanol.

not affect the fitting of the experimental data and the predictions of the dynamic model, as has been verified by computer simulations.

In essence, the macroscopic kinetic model can be summarized by the following key steps: (I) macromixing leads to a growth of the organic/aqueous interface accompanied by a slow transformation of EC into C at the interface; (II) C forms aggregates by which EC is simultaneously captured and temporarily stored in a micelle-EC complex (MEC); (3) these transient aggregates transport EC into the aqueous phase, allowing the rapid alkaline hydrolysis of EC within the aqueous phase. This last process gives rise to an accelerating growth in the concentration of C. All these steps are considered as reversible processes that can interact with each other. The resulting kinetic model is shown in Scheme 1.

Step I. The first step of the model scheme represents roughly the reversible growth of the macroscopic organic/aqueous interface by the influence of mixing.²⁹ In this case the bulk organic phase (EC_{org}) breaks down into small liquid droplets, leading to an increase in the surface area in contact with the aqueous phase (EC_{int}). Only this portion of the total EC was

assumed to be available for further chemical processes, while EC_{org} was treated as an inactive chemical reservoir. Altering the value of k_1 may simulate changes in the growth of the organic/aqueous interface such as that caused by increasing the intensity of stirring.

Step II. This step describes the slow spontaneous hydrolysis of EC occurring at the organic/aqueous interface yielding caprylate monomers and ethanol (EtOH), both of which accumulate in the aqueous phase.³⁰ Obviously, this process is controlled by the amount of EC_{int} supplied by step I (i.e., the stirring rate).

Step III. This step accounts for the reversible process of aggregation ($g = 40$). This process represents an oversimplification when compared to a multistep approach. However, as already mentioned, the one-step approach and the assumption of micellar monodispersity has been found to be sufficient for our objectives of a macroscopic dynamic description. Indeed, as shown in Figure 4, the theory suggests that micelles are very narrowly dispersed. The value for the equilibrium constant of step III has been adjusted to reproduce the experimentally measured cmc and is in accordance with the value predicted by the a priori theory (Appendix I).

Steps IV and V. These processes denote formally the dissolution of an average of p molecules of EC by each micelle occurring at the organic/aqueous interface and their transport into the aqueous phase by MEC. The value of $p = 5$ has been chosen based on the experimentally observed dissolution of EC in sodium caprylate micelles (see Figure 3), taking into account $g = 40$. In particular, steps IV and V resemble in some respect the process of a phase-transfer catalysis.

Step VI. This step takes account of the hydrolysis of EC transported into the aqueous phase. The process is assumed to be faster than the hydrolysis occurring at the interface (step II), since EC_{aq} is entirely surrounded by OH⁻.

IV. Validation and Discussion

As shown in Figure 1, the numerical least-squares fitting of the experimentally observed time evolution of EC and total C by the model shows excellent agreement. This result illustrates the capacity of the model scheme to represent the overall dynamics of the reaction system with good accuracy (see Appendix II for details about the computations).

Starting from this fitting of experimental data, the model enables us to also simulate the effect of initial addition of sodium caprylate, which we have measured experimentally (see Figure 5). As expected, experiments show that the initial addition of sodium caprylate reduces the total reaction time. Our simulation gives similar results. The discrepancy between experimental and simulated results can be attributed to the fact that the experimental setup used to obtain the measurements plotted in Figure 5 differs significantly from the setup used to obtain the data in Figure 1, which is the basis for the parameters used in the simulation.

The stirring intensity affects strongly the duration of the induction period as shown in ref 3 and by our own experiments. This behavior can also be predicted qualitatively by altering the value of k_1 and keeping all the other kinetic parameters as obtained by the fitting shown in Figure 1. When k_1 is decreased, the kinetic curve of C (Figure 6) becomes very similar to that given by Bachmann, Luisi, and Lang.³ As shown by the enlargement in Figure 6, this kinetic curve obeys the same specific shape and slope in the domain of rapid C formation as seen in our experiment (Figure 1).

The main dynamic features of the kinetic model are revealed by the time evolution of M and MEC, which were obtained by

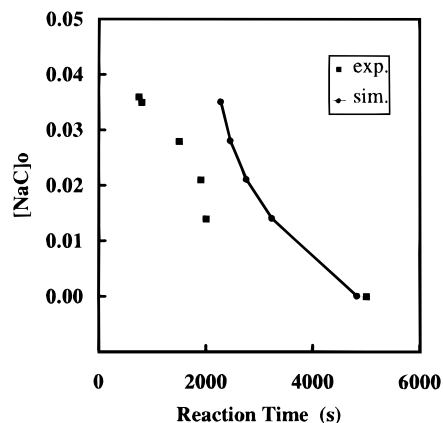


Figure 5. Effect of initial addition of sodium caprylate (NaC) on the total reaction time of the biphasic alkaline hydrolysis of EC: (■, exp.) experimentally measured (note that the experimental setup for these measurements differs from that of the experiment shown in Figure 1; see section VI for details); (●, sim.) predicted by the kinetic model by using the kinetic parameters obtained by the fitting of the experiment shown in Figure 1.

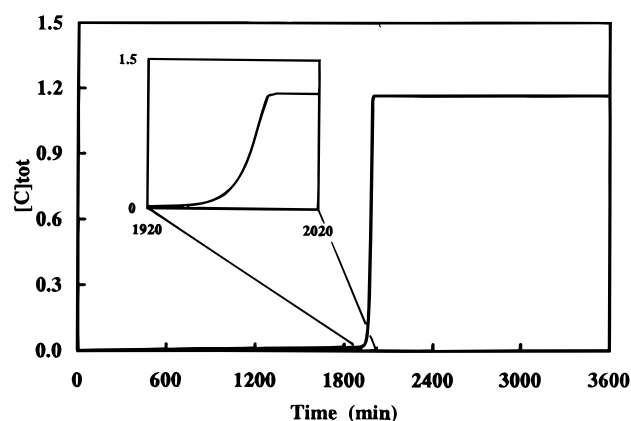


Figure 6. Simulation of the time evolution of total [C] when $k_1 = 1.9 \times 10^3 \text{ min}^{-1}$ (all other kinetic parameters are the same as those used for the fitting of experimental data; see Figure 1 and Appendix II). Note that the enlargement of the curve in the region between 1920 and 2020 min shows the similar specific curvature as shown in Figure 1.

simulations on the basis of the kinetic constants estimated via experimental data fitting. In particular, the model shows that the formation of the micelle-EC complex (MEC) is more favorable compared to that of the pure micelles (M). This is entirely consistent with the phenomenon of solubilization in micellar systems.²⁸ When a solubilize is available, solubilize-containing micelles rather than pure micelles are formed.

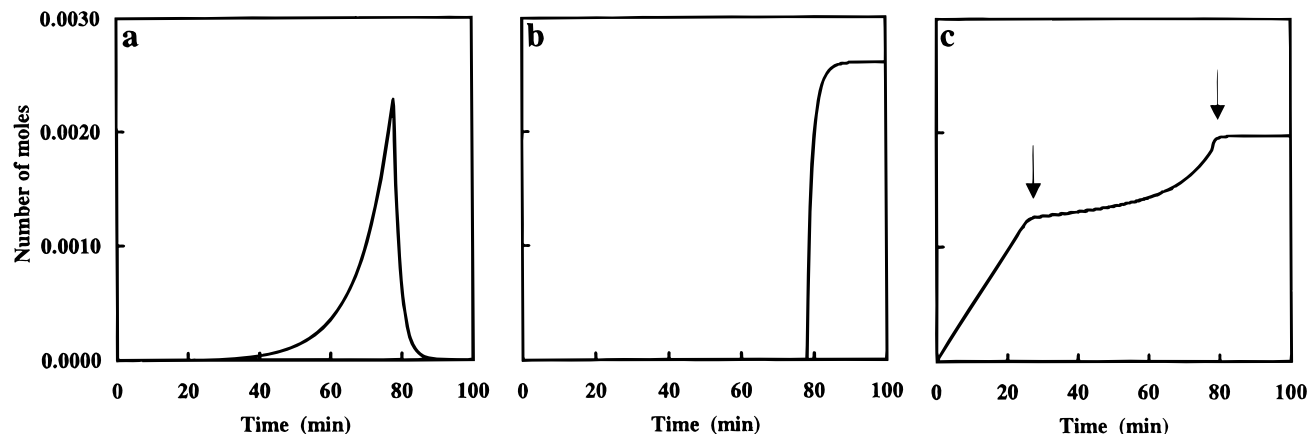


Figure 7. Simulation of the time evolution of MEC (a), M (b), and C (c) by the kinetic model using the kinetic parameters obtained by the fitting of the experiment shown in Figure 1 (total reaction volume is 0.091 L). Note the two characteristic points during the time evolution of C.

Consequently, as long as any EC is available, only MEC is produced, and the formation of M occurs only when EC is completely depleted (see parts a and b of Figure 7). The time evolution of the caprylate monomer concentration shows two characteristic points: one corresponding to the critical aggregate concentration (cac) of MEC at $[C] \approx 1.3 \times 10^{-2} \text{ mol L}^{-1}$ and the second corresponding to the cmc of M at $[C] \approx 2 \times 10^{-2} \text{ mol L}^{-1}$ (Figure 7c). The formation of solubilize-containing micelles occurs at a critical concentration that is smaller than the cmc associated with the formation of the pure micelles. Hence, we deal with two completely different species: MEC and M. The first is a reactive intermediate that acts like a phase-transfer catalyst, and the second is a kinetically inactive product of the reaction. The occurrence of two critical concentrations (cac and cmc) also shows that the process of solubilization, i.e., the formation of MEC, affects the aggregation process. Note also that according to our model, the autocatalytic stage of the reaction starts *before* [C] has reached the cmc.

The model assumption of a phase-transfer process leads to an acceptable description of the experimentally observed kinetics (i.e., the comparatively smooth increase and the abrupt end of the overall process and also of the solubilization of EC in the micellar phase (Figure 3b)). Applying a model scheme without MEC and assuming a direct micellar catalysis, we failed to fit the experimental data reported in this paper. Such models without the implication of transport phenomena that have been proposed so far are not able to reproduce the specific curvature (i.e., the smooth increase of C formation followed by an abrupt cutoff of the reaction), as seen in our experiment (Figure 1) no matter what values for the kinetic parameters have been employed. The kinetic data given in ref 3 are not adequate for discriminating between a model with and without the involvement of MEC.

V. Conclusion

In this paper we have presented a macroscopic kinetic model to account for the overall dynamics of the biphasic alkaline hydrolysis of EC. This model was validated by close fitting of the experimentally observed time evolution of EC and total [C].

Based on this model, the overall process of the reaction can be understood in the following terms. In the first (hydrodynamically controlled) stage of reaction the organic/aqueous interface increases because of mixing. C is slowly produced and accumulates in the aqueous phase. The concentration of C reaches the cac at which the formation of MEC starts. These aggregates temporarily store EC and transport it into the aqueous phase, where rapid hydrolysis takes place. Pure micelles are

formed as a final product when EC is totally consumed. Steps IV and V of the model scheme, denoting a process similar to a phase-transfer catalysis, must be regarded as the key dynamics of the overall reaction.

An important question is whether we are really dealing with a process that has been designated as “micellar autocatalysis”. We have shown that, according to our model, pure micelles have no kinetic effect on the reaction process because they are formed when the reaction is almost finished. A basic dynamic feature originates from the biphasic character of the reaction system. Hence, the nonlinear dynamic behavior is explained in terms of a transport phenomenon of a phase-transfer type rather than in terms of micellar catalysis, which—in addition to this—is chemically less realistic. In this respect, it is interesting to note that nonlinear effects in the course of phase-transfer catalysis have already been described about 20 years ago.³¹ On the other hand, kinetic curves indicating highly autocatalytic effects in biphasic vesicular systems have been reported⁵ and more recently analyzed by a type A kinetic model.³² These kinetic curves show characteristics very similar to those we have found for the biphasic alkaline hydrolysis of EC. This may point out that a transport phenomenon (as described by our model) takes place in these reaction systems as well.

VI. Experimental Section

Reagents. For all experiments commercial products were used without further purification: ethyl caprylate, >98% (Fluka); sodium caprylate, >99% (Fluka); sodium hydroxide, p.a. (Prolabo); *n*-pentanol, p.a. (Prolabo); ethanol, p.a. (Merck); sodium chloride, p.a. (Prolabo). For aqueous solutions doubly distilled water has been used.

Alkaline Hydrolysis of EC. The reaction was performed under reflux in a thermostated 250 mL round-bottom glass flask at 90 °C by vigorous mixing of the two liquid phases (consisting of 70 mL aqueous 3 M NaOH and 21 mL neat EC) with a magnetic bar of 25 mm × 6 mm size at about 800 rpm.

Determination of EC and C. At fixed time intervals the quantity of EC was determined by volumetric measurements of the actual organic phase. The concentration of C was determined by IR spectroscopy at ~1560 cm⁻¹ using a Perkin-Elmer 683 instrument equipped with 0.05 mm CaF₂ cells. For this measurement 50 μL aliquots of the aqueous phase of the reaction mixture were withdrawn, cooled at 25 °C, diluted with 1 mL *n*-pentanol, and then transferred into the IR cells.

Measurement of cmc. The cmc of sodium caprylate was determined by using a thermostated Prolabo Tensimat apparatus at 25 °C. A variation of the cmc with temperature was not considered but assumed to be small. This assumption is in agreement with the prediction of the cmc at 90 °C (0.025 M) by the a priori theory (see Appendix I).

Solubility of EC in Micellar Phase. This was determined at 25 °C after a procedure already described in ref 3. We assumed that the reaction temperature of 90 °C does not affect significantly the solubility of EC in the micellar phase.

Initial Addition of Sodium Caprylate. Experiments have been performed in a well-stirred and thermostated (90 °C) quartz cuvette of 2.1 mL total volume equipped with a simple air-cooled reflux unit. The total reaction time has been set equal to the point where the reaction mixtures become entirely transparent (total consumption of the organic phase), which has been recorded by UV-vis spectroscopy at λ = 300 nm with an HP 8451 diode array spectrophotometer.

Computations. Model calculations were performed on a workstation (HP 9000-710). The general simulation and optimization procedures were performed by using a nonlinear

minimization algorithm for the fitting of the model to the experimental data³³ and by using a semiimplicit Runge–Kutta method^{34–36} for the numerical integration.

Appendix I: Predicting the Micellization Behavior of Sodium Caprylate

The aggregation characteristics of sodium caprylate (C₇H₁₅-COONa), including the cmc, the average aggregation number of micelles, the variance of the micelle size distribution, and the micellization equilibrium constant (step III of Scheme 1), can be predicted a priori using the molecular thermodynamic theory formulated by Nagarajan and Ruckenstein.²⁶ For a surfactant solution containing micelles of various aggregation numbers *g*, the Gibbs equilibrium condition stipulates that the chemical potential of a molecule in an aggregate of size *g* must be equal to the chemical potential of a singly dispersed molecule:

$$\mu_g^\circ + kT \ln X_g = g(\mu_1^\circ + kT \ln X_1)$$

Here, *X*₁ and *X*_{*g*} are the mole fractions of the singly dispersed molecules and the aggregates of size *g*, respectively, and μ_1° and μ_g° are their respective standard chemical potentials corresponding to those of infinitely dilute solution conditions. The total surfactant concentration is calculated as $X_{\text{tot}} = X_1 + \sum gX_g$. The mole fractions *X* are readily converted to molar concentrations of C by multiplying by 55.5.

To calculate the micelle size distribution *X*_{*g*} versus *g* using the above equation, we need an explicit expression for $\Delta\mu_g^\circ = (\mu_g^\circ/g) - \mu_1^\circ$, which is the difference between the standard chemical potentials of a surfactant molecule in an aggregate of size *g* and a singly dispersed surfactant molecule in the solvent, as a function of the size and shape of the micelles. Micelles of small aggregation numbers pack as spheres, while larger micelles pack into globular or ellipsoidal shapes. All the geometrical properties of the spherical and ellipsoidal micelles are dependent only on the aggregation number *g*. These relations are given in ref 26. The standard chemical potential difference term $\Delta\mu_g^\circ$ is the sum of the number of contributions that have been identified by considering the changes in the intermolecular interactions accompanying the micellization process. Specifically, these contributions account for the following factors. (a) The surfactant tail is removed from contact with water and is transferred to the hydrophobic core of the micelle ($\Delta\mu_g^\circ$)_{tr}. The presence of large amounts of added electrolyte influences this transfer process. This free energy contribution is independent of the aggregation number *g*. All the other free energy contributions listed below are dependent on the size and shape of the micelles. (b) The surfactant tail inside the micelle has a conformation different from that in a pure hydrocarbon liquid because of packing constraints imposed inside the micelle ($\Delta\mu_g^\circ$)_{def}. (c) The formation of the micelle creates an interface between the hydrophobic micellar core and the solvent ($\Delta\mu_g^\circ$)_{int}. (d) The polar head groups of the surfactants at the micelle surface exhibit steric repulsions ($\Delta\mu_g^\circ$)_{ste}. (e) The polar head groups, if they are ionic, also exhibit at the micelle surface mutual electrostatic repulsions ($\Delta\mu_g^\circ$)_{ionic}. Expressions for each of these free energy contributions have been developed in ref 26 as functions of temperature *T*, the molar concentration of added electrolyte *C*_{add}, and the micellar aggregation number *g*.

The molecular constants necessary for the predictive calculations are estimated from the molecular structure of sodium caprylate. Only two molecular constants, which are specific for a given ionic head group of the surfactant, are needed. One is the cross-sectional area *a*_p of the head group, which is estimated to be 0.11 nm² for sodium carboxylate. The other is

the distance from the hydrophobic core surface to the position where the counterion Na^+ is located, which is estimated to be $\delta = 0.555$ nm. The molecular volume v_s and the extended length l_s of the surfactant tail consisting of n_c carbon atoms are calculated from the group contributions of methylene and methyl groups given in ref 26.

The micellization behavior of sodium caprylate is predicted at the experimental conditions of 90 °C and 3 M NaCl in the surfactant solution. The cmc is predicted to be 0.0245 M based on a sharp transition in the plot of X_1 against the total concentration X_{tot} . The cmc predicted in the absence of any NaCl at 90 °C is 0.445 M. The predicted size distribution X_g as a function of the aggregation number g is plotted in Figure 4 for three values of the total surfactant concentration: 0.026, 0.0576, and 0.1045 M. The predicted weight-average aggregation number $g_w (= \sum g^2 X_g / (\sum g X_g))$ is 39 when the total surfactant concentration is 0.025 M and 42 when the concentration is 0.10 M. The predicted variance in the size distribution σ is $0.25g_w$. The monomer-micelle equilibrium constant k_3/k_{-3} describing step III of Scheme 1 is equal to $[\exp(-g\Delta\mu_g^\circ/kT)/(55.5)^{g-1}]$. This is predicted by the model to be 2×10^{62} if $g = 41$ and 3×10^{59} if $g = 39$.

Appendix II: Differential Equations and Parameters of the Kinetic Model

The six-step kinetic model shown in Scheme 1 consists of eight species of which ethanol (EtOH) is regarded as an inactive final product, which consequently is not considered for further computational treatment. Because of the nonhomogeneous (biphasic) character of the reaction system, the total quantities of each species are expressed in number of moles (indicated by capital letters) instead of concentrations (indicated by square brackets).

The rate constants k are expressed by usual units, i.e., for monomolecular reactions in min^{-1} ($k_I, k_{-I}, k_{-III}, k_{-IV}, k_V$), for bimolecular reactions in $\text{mol}^{-1} \text{L min}^{-1}$ ($k_{II}, k_{IV}, k_{-V}, k_{VI}$), and for n -molecular reactions in $\text{mol}^{1-n} \text{L}^{n-1} \text{min}^{-1}$ (k_{III}). The reaction fluxes r , presented as follows, are multiplied by $V^{(1-n)}$ (V is the volume of the aqueous phase) for reactions with $n > 1$, which leads to an entire representation in the units mol min^{-1} :

$$\begin{aligned} r_I &= k_I \times \text{EC}_{\text{org}} \\ r_{-I} &= k_{-I} \times \text{EC}_{\text{int}} \\ r_{II} &= (k_{II} V^{-1}) \times \text{EC}_{\text{int}} \times \text{OH}^- \\ r_{III} &= (k_{III} V^{1-g}) \times C^g \\ r_{-III} &= k_{-III} M \\ r_{IV} &= (k_{IV} V^{-1}) \times M \times \text{EC}_{\text{int}} \\ r_{-IV} &= k_{-IV} \times \text{MEC} \\ r_V &= k_V \times \text{MEC} \\ r_{-V} &= (k_{-V} V^{-1}) \times M \times \text{EC}_{\text{aq}} \\ r_{VI} &= (k_{VI} V^{-1}) \times \text{EC}_{\text{aq}} \times \text{OH}^- \end{aligned}$$

Here, g denotes the mean aggregation number of the micelles. The volume of the aqueous phase has been calculated by using

$$V = V_{\text{tot}} - (\text{EC}_{\text{org}} + \text{EC}_{\text{int}}) V_{\text{mol}}$$

where V_{mol} is the molar volume of EC, and V_{tot} the total volume of the reaction mixture, which has been considered to remain constant.

The respective kinetic equations that have been used for the numerical calculations are given as follows:

$$\begin{aligned} d(\text{EC}_{\text{org}})/dt &= -r_I + r_{-I} \\ d(\text{EC}_{\text{int}})/dt &= r_I - r_{-I} - r_{II} + p(r_{-IV} - r_{IV}) \\ d(\text{OH}^-)/dt &= -r_{II} - r_{VI} \\ d(C)/dt &= g(r_{-III} - r_{III}) + r_{VI} + r_{II} \\ d(M)/dt &= r_{III} - r_{-III} - r_{IV} + r_{-IV} + r_V - r_{-V} \\ d(\text{MEC})/dt &= r_{IV} - r_{-IV} - r_V + r_{-V} \\ d(\text{EC}_{\text{aq}})/dt &= p(r_V - r_{-V}) - r_{VI} \end{aligned}$$

Here, p denotes the average number of molecules of EC per MEC. For the sake of simplicity p is not considered to count for the reaction order of the respective processes r_{IV} and r_{-V} (consequently, both processes are treated as second order).

The starting values used for the computations were $\text{EC}_{\text{org}0} = 0.106$ mol, $\text{OH}^-_0 = 0.21$ mol, $V_{\text{tot}} = 0.091$ L, $V_{\text{mol}} = 0.198$ L mol^{-1} .

After $g = 40$ and $p = 5$ were preset, the numerical values for the kinetic parameters obtained by the fitting of the experimental data as shown in Figure 1 are

$$\begin{aligned} k_I &= 6.6 \times 10^6 \text{ min}^{-1} \\ k_{-I} &= 1.7 \times 10^5 \text{ min}^{-1} \\ k_{II} &= 1.6 \times 10^{-4} \text{ mol}^{-1} \text{ L min}^{-1} \\ k_{III} &= 10^{64} \text{ mol}^{-39} \text{ L}^{39} \text{ min}^{-1} \\ k_{-III} &= 1 \text{ min}^{-1} \\ k_{IV} &= 2.6 \times 10^{13} \text{ mol}^{-1} \text{ L min}^{-1} \\ k_{-IV} &= 7.5 \times 10^7 \text{ min}^{-1} \\ k_V &= 8.4 \times 10^{-1} \text{ min}^{-1} \\ k_{-V} &= 2.4 \times 10^5 \text{ mol}^{-1} \text{ L min}^{-1} \\ k_{VI} &= 4.3 \times 10^4 \text{ mol}^{-1} \text{ L min}^{-1} \end{aligned}$$

The parameters k_I, k_{-I} , and k_{II} represent an ensemble that can be assigned to the induction period of the reaction. All these parameters determine the actual quantity of EC_{int} where the product of $k_{II} \times \text{EC}_{\text{int}}$ controls the rate of the spontaneous hydrolysis of EC (i.e., the consumption of EC_{int}) and k_I is related to the effect of stirring. For the micellization process, the value of the ratio k_{III}/k_{-III} has been adjusted in order to obtain a cmc of 0.02 mol L^{-1} . This value is in agreement with the predictions of the a priori theory (see Appendix I). The parameters k_{IV}, k_{-IV}, k_V , and k_{-V} constitute a second ensemble involved in the fast part of the reaction. They can be regarded as two equilibria that are directed to the formation of MEC, ensuring its accumulation (which is in agreement with the phenomenon of

solubilization in micellar systems). The fast hydrolysis is determined by the value of k_{VI} , which must be $\geq 4.3 \times 10^4 \text{ mol}^{-1} \text{ L min}^{-1}$ for optimal data fitting.

For the comparison of the computational results with the experimental data the following expression has been used:

$$[C]_{\text{tot}} = \{C + g(M + \text{MEC})\}/V$$

where $[C]_{\text{tot}}$ is the total caprylate concentration in mol L^{-1} .

References and Notes

- (1) Bachmann, P. A.; Walde, P.; Luisi, P. L.; Lang, J. *J. Am. Chem. Soc.* **1990**, *112*, 8200.
- (2) Bachmann, P. A.; Walde, P.; Luisi, P. L.; Lang, J. *J. Am. Chem. Soc.* **1991**, *113*, 8204.
- (3) Bachmann, P. A.; Luisi, P. L.; Lang, J. *Nature* **1992**, *357*, 57.
- (4) Hadlington, S. *Chem. Br.* **1992**, *28*, 10.
- (5) Walde, P.; Wick, R.; Fresta, M.; Mangone, A.; Luisi, P. L. *J. Am. Chem. Soc.* **1994**, *116*, 11649.
- (6) Luisi, P. L.; Walde, P.; Oberholzer, T. *Ber. Bunsen-Ges. Phys. Chem.* **1994**, *98*, 1160.
- (7) Walde, P.; Goto, A.; Monnard, P. A.; Wessicken, M.; Luisi, P. L. *J. Am. Chem. Soc.* **1994**, *116*, 7541.
- (8) Kust, P. R.; Rathman, J. F. *Langmuir* **1995**, *11*, 3007.
- (9) Menger, F. M.; Portnoy, C. E. *J. Am. Chem. Soc.* **1967**, *89*, 4698.
- (10) Menger, F. M.; Portnoy, C. E. *J. Am. Chem. Soc.* **1968**, *90*, 1875.
- (11) Fendler, J. H.; Fendler, E. J. *Catalysis in Micellar and Macromolecular Systems*; Academic Press: New York, 1975.
- (12) Marconi, D. M. O.; Frescura, V. L. A.; Nome, F.; Bunton, C. A. *J. Phys. Chem.* **1994**, *98*, 12415.
- (13) Billingham, J.; Coveney, P. V. *J. Chem. Soc., Faraday Trans.* **1994**, *90*, 1953.
- (14) Chizmadzhev, Y. A.; Maestro, M.; Mavelli, F. *Chem. Phys. Lett.* **1994**, *226*, 56.
- (15) Coveney, P. V.; Wattis, J. A. D. *Proc. R. Soc. London, Ser. A* **1996**, *452*, 2076.
- (16) Recently Coveney et al. reported in a purely theoretical paper the simulation of the biphasic hydrolysis of ethyl caprylate by the use of a lattice-gas automaton (Coveney, P. V.; Emerton, A. N.; Boghosian, B. M. *J. Am. Chem. Soc.* **1996**, *118*, 10719).
- (17) A similar model of a surface-controlled reaction has been recently proposed by Mavelli and Luisi for the kinetic description of "autopoietic self-reproduction of vesicles" in a biphasic system (ref 32).
- (18) Gray, P.; Scott, S. K. *Chemical Oscillations and Instabilities*; Clarendon Press: Oxford, 1990.
- (19) Billingham, J.; Needham, D. J. *Philos. Trans. R. Soc. London A* **1992**, *340*, 569.
- (20) Becker, R.; Döring, W. *Ann. Phys.* **1935**, *24*, 719.
- (21) Wall, S. N. *J. Phys. Chem.* **1974**, *78*, 1024.
- (22) Aniansson, E. A. G.; Wall, S. N.; Almgren, M.; Hoffmann, H.; Kielmann, I.; Ulbricht, W.; Zana, R.; Lang, J.; Tondre, C. *J. Phys. Chem.* **1976**, *80*, 905.
- (23) Wall, S. N.; Aniansson, G. E. A. *J. Phys. Chem.* **1980**, *84*, 727.
- (24) Kresheck, G. C.; Hamori, E.; Davenport, G.; Scheraga, H. A. *J. Am. Chem. Soc.* **1966**, *88*, 246.
- (25) The reaction mixture becomes deeply turbid and gray just before becoming abruptly transparent when the reaction is finished. This observation can be interpreted by the proposed kinetic model as the formation of the micelle-EC complex (MEC); see also section IV.
- (26) Nagarajan, R.; Ruckenstein, E. *Langmuir* **1991**, *7*, 2934.
- (27) Rosenholm, J. B.; Gigg, R. B.; Hepler, L. G. In *Solution Behavior of Surfactants*; Mittal, K. L., Fendler, E. J., Eds.; Plenum Press: New York, 1982; Vol. 1, pp 359-371.
- (28) Attwood, D.; Florence, A. T. *Surfactant Systems*; Chapman and Hall: London, 1983.
- (29) Experiments show that the influence of stirring affects the induction period but not the shape and the slope of the autocatalytic part of the kinetic curve.
- (30) Because of their amphiphilic nature it is known that C_{aq} will preferably adsorb at the organic/aqueous interface with the polar head groups orientated toward the aqueous phase and the nonpolar tails toward the organic phase. This process has been tested by including the following step in the model: $EC_{\text{int}} + C \rightleftharpoons [\text{cover}]$, where [cover] denotes the amount of liquid/liquid interface that is no longer available for process II, since it is blocked by C (resulting in an inhibition of the hydrolysis reaction). The above shown process also inhibits the fusion of EC_{int} , i.e., the back-reaction of step I, which is reasonable and which has been verified experimentally. We found that small amounts of sodium caprylate slow down significantly the phase separation of an aqueous/EC system. Nevertheless, the formation of [cover] does not change the capacity of the model to describe the experimentally observed kinetics of the overall system and does not improve the fitting of experimental data. For this reason this process has been omitted in Scheme 1.
- (31) Starks, C. M.; Owens, R. M. *J. Am. Chem. Soc.* **1973**, *95*, 3613.
- (32) Mavelli, F.; Luisi, P. L. *J. Phys. Chem.* **1996**, *100*, 16600.
- (33) Minoux, M. *Programmation Mathématique. Tome 1*; Dunod: Paris, 1983; Chapter 4 (ISBN 2-04-0.15487-6).
- (34) Kaps, K.; Rentrop, P. *Numer. Math.* **1979**, *33*, 55.
- (35) Gottwald, B. A.; Wanner, G. *Computing* **1981**, *26*, 355.
- (36) Kaps, K.; Rentrop, P. *Comput. Chem. Eng.* **1984**, *8*, 393.